Effect of Ambient Pressure on the Extinction Limit for Opposed Flame Spread over an Electrical Wire in Microgravity

Masashi Nagachi[a], Jean-Marie Citerne[b], Hugo Dutilleul[b], Augustin Guibaud[b]

Grunde Jomaas[c], Guillaume Legros[b], Nozomu Hashimoto[a], Osamu Fujita[a*]

[a]Hokkaido University, Sapporo, Hokkaido, 066-8628, Japan
[b]Sorbonne Université, CNRS, UMR 7190, Institut Jean Le Rond d'Alembert, Paris F-75005, France
[c]School of Engineering, University of Edinburgh, EH9 3FG, Edinburgh, United Kingdom

[*]Corresponding author. Fax: +81 11706 7841. E-mail address: ofujita@eng.hokudai.ac.jp (O. Fujita).

Colloquium: Fire research

Total length of the paper: 5818 / 6200

Equations: 192
Main text: 3307
References: 577
Figure 1: 442
Figure 2: 167
Figure 3: 169
Figure 4: 171
Figure 5: 164
Figure 6: 464
Figure 7: 165

Abstract (247 / 100~300)

Parabolic flight experiments were carried out to investigate the effect of ambient pressure on the extinction limit for opposed flame spread over an electric wire insulation in microgravity. Low-density polyethylene insulated Nickel-Chrome wires with inner core diameter of 0.50 mm and insulation thickness of 0.30 mm were examined for ambient pressures ranging from 50 kPa to 140 kPa for an external opposed flow of 10 cm/s. The experiments showed that the limiting volumetric oxygen concentration (LOC) increased as the total ambient pressure decreased. This LOC trend can be explained by radiation loss from wire surface. The radiation loss increased as the ambient pressure decreased – a result that can be explained by the increase in preheat length with decreasing ambient pressure. Moreover, when the data was plotted in a partial pressure vs. total pressure space, it became evident that the limiting oxygen partial pressure (LOPP) decreased with decreasing total ambient pressure. This LOPP trend can be explained by the fact that the flame temperature increased as the ambient pressure decreased under constant oxygen partial pressure. In current fire safety design for spacecraft, tentative oxygen concentration criteria in spacecraft suggested by NASA is assumed as 30% of oxygen concentration, and this value is assumed independent of ambient pressure. However, the present result implies that consideration of the effect of ambient pressure on the flammability limit is necessary, especially with respect to the possibility of an extension of the allowable atmosphere condition for spacecraft cabin in the low pressure region.

Keywords

Ambient pressure; Opposed flame spread; Microgravity; Electrical wire; Fire safety in space

1. Introduction

Fire safety in spacecrafts is one of the most important requirements for manned space missions [1]. A likely fire cause in spacecrafts is ignition and flame spread over the wire insulation that is used in the numerous electric devices. Moreover, numerous studies showed that combustion phenomena in microgravity are different from normal gravity phenomena, especially due to the absence of buoyancy [2, 3]. Therefore, it is important to understand the ignition and flame spread behavior on wire insulation in microgravity, especially in the environmental conditions associated with spacecraft. Many of the important aspects related to the flammability of wire insulation in microgravity have already been studied for numerous materials and conditions; the ignition limit [4–6], the flame spread rate [7–16], and the extinction limit [17–21]. However, there are very few research results for flame spread over wire insulation in microgravity at various ambient pressure conditions. This is somewhat surprising, as a low pressure, high oxygen concentration, as compared with sea-level conditions, was suggested for spacecraft to prevent decompression sickness and to be suitable for the human living environment [22]. A similar suggestion with more details was given in NASA/TP-2019-220232 [23].

Several reports have shown that combustion phenomena were affected by ambient pressure. Honda et al. [24] summarized the experimental data of flame spreading over flat sheet in normal gravity (downward spreading) and microgravity using various diluent gas and showed that the flame spread rate decreased as ambient pressure decreased because of increasing of radiation loss. Thomsen et al. conducted the experiments about concurrent flame spread (upward spreading) over Nomex sheet in

normal gravity, and showed that the flame spread rate decreased as ambient pressure decreased because of reduction of buoyancy [25]. Also, they conducted the experiments to figure out the effect of ambient pressure on downward flame spread limit in normal gravity, and showed that limiting oxygen concentration of spreading flame increased as ambient pressure decreased [26]. Similar phenomena were observed in normal gravity, even for different materials, shapes and direction of air flow [27, 28]. In terms of wire cases, Kikuchi et al. conducted experiments in microgravity using the 10 s drop tower to assess the pressure effect on flame spreading over ETFE-coated wire insulation in quiescent atmosphere, which showed that the flammable range of pressure was narrower under microgravity than that in normal gravity [10]. However, they performed experiments under only one ambient oxygen concentration, therefore could not discuss about the effect of ambient pressure on limiting oxygen concentration of the spreading flame studied. Nakamura et al. reported that the effect of ambient pressure on flame spreading over horizontal setting wire in terms of flame spread rate in normal gravity [14]. Moreover, Fang et al. conducted experiments in normal gravity to discuss the effect of low ambient pressure on dripping and extinction limit of flame spread over wire insulation in quiescent condition [29]. However, this research had been conducted at normal gravity and this phenomenon was controlled by natural convection. As a result, the findings could not be extended to the effect of ambient pressure in microgravity. Therefore, in our best knowledge, there is still limited research to assess the pressure effect on flame spreading over wire insulation in microgravity.

The present investigation focuses on the relationship between ambient pressure and the extinction limit for opposed flame spread over wire insulation in microgravity (obtained by the means of parabolic flights). Also, the discussion about the effect of ambient pressure on the extinction limit is conducted based on scaling analysis using the energy balance for the wire configuration.

2. Experimental configuration

The Detection of Ignition and Adaptive Mitigation Onboard for Non-Damaged Spacecrafts (DIAMONDS) rig developed by Sorbonne Universite´ (Paris, France) and the French Space Agency (CNES) was operated to conduct the investigations. A detailed description of the experimental design and method and further information is available from Citerne et al. [9]. The cylindrical part of chamber has an inner diameter of 190 mm. In the combustion chamber, the oxidizer flow enters from the bottom and is vented at the top. The oxidizer velocity and composition is controlled by mass flow controllers. A backlight probing the spreading flame is turned on/off with fixed intervals. As a result, the camera located on the opposite side not only captures the direct flame emission, but also the image with the backlight, which is used to visualize the behavior of molten insulation and the soot distribution in the flame. The oxygen concentration in the oxidizer flow can be adjusted from 0 to 21 % by mixing of air and nitrogen gas.

In this experiment, the external flow velocity inside the chamber was always set to 10 cm/s and the pressure inside the chamber could be adjusted from 50 to 140 kPa. Moreover, a low-density polyethylene (LDPE) insulated Nickel-Chrome (NiCr) wire was systematically used. LDPE is a

laboratory material, which has always been used for scientific discussion of wire combustion. A natural next step in this research is to use a practical material such as ETFE. The core diameter and the insulation thickness were 0.5 mm and 0.3 mm, respectively. This configuration aligns with previously reported experiments [20]. Every sample holder had a wire coated with LDPE over a length of 130 mm. Each sample holder was placed along the center line of the chamber. For the ignition procedure, an 8 mm coil made from 0.5 mm diameter Kanthal wire was wrapped around (6 turns) the downstream end of the sample wire, and the coil produced approximately 94 W for 8 seconds. The ignition sequence was initiated before the start of the microgravity period, so that the actual ignition occurred during microgravity. The microgravity experiments were carried out during CNES parabolic flights on board of the Novespace A310 airplane, which enables microgravity conditions for about 22 s with a gravity level lower than 10^{-2} g_0 (g_0 = 9.81 ms^{-2}) for each parabola.

3. Results

Overall, the experiments yielded many interesting and novel results. In the following, the details of the flame appearance and the extinction limit will be presented. A deeper analysis and discussion then follows in Section 4.

3.1. Flame appearance

Figure 1 shows typical flame images in microgravity at constant oxygen concentration and various ambient pressure levels. Also, the flame images at normal gravity are shown for comparison. In these images, the external oxidizer stream flows from the bottom to the top, and the direction of the

spreading flame is opposed.

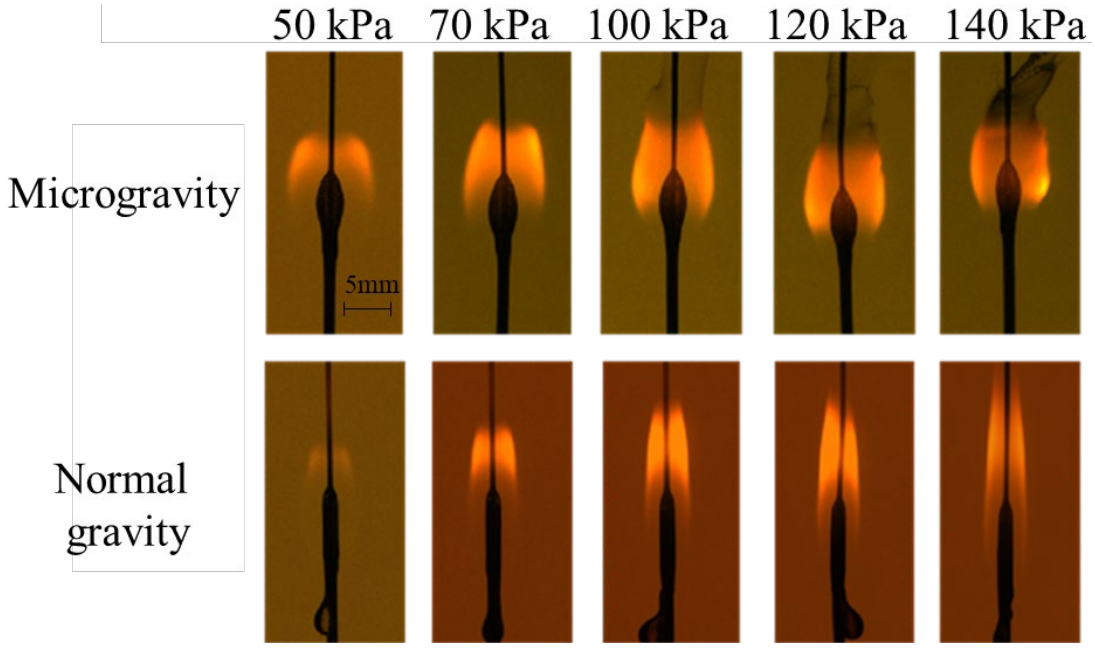

Fig. 1 Backlighted images of opposed flame spread over wire insulation at different ambient pressures
(21 % of oxygen concentration, 100 mm/s of external flow velocity)

As expected based on theory and previously reported results, the flames assumed a rounded shape in microgravity, whereas the flames assumed a stretched shape at normal gravity (see Fig. 1). Also, significant amount of soot was produced in microgravity as compared to normal gravity, and the amount of soot was enhanced as ambient pressure increased, as evidenced by the darker plume in high pressure case. Further investigations to measure the distributions of soot volume fraction and temperature were conducted by Guibaud et al.[30–32].

3.2. Extinction limit

In this study, when a flame was sustained during the whole microgravity period of each experiment, it was considered as a "propagation" scenario. When a flame was not sustained during the whole period of microgravity, it was considered as an “extinction” scenario. Near the extinction

limit condition, the flame luminosity was too dim to be captured by the camera. Therefore, the propagation/extinction status was determined by the movement of the molten insulation in the flame using the backlighted frames. Then, the extinction limit was assumed to exist between the maximum extinction case and the minimum propagation case. Figure 2 shows the extinction limit using volumetric oxygen concentration (Limiting Oxygen Concentration: LOC) of flame spread over a wire insulation in microgravity under different total ambient pressure conditions.

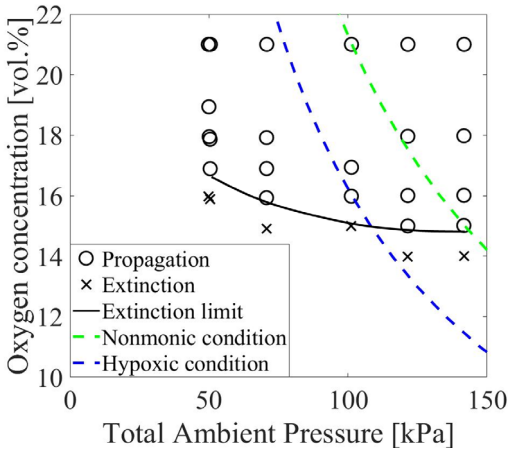

Fig. 2 Extinction limit using volumetric oxygen concentration
(Flow velocity: 10 cm/s, opposed flow, microgravity)

This dataset is extracted from single run experiments for each plot. An open circle shows flame propagation conditions, and a cross shows flame extinction conditions. Also, the solid line shows the LOC expected from the experimental results. According to Fig. 2, the LOC increased as the ambient pressure decreased. It means that low pressure region has an advantage regarding material flammability.

However, considering fire safety for manned spacecraft, information of oxygen partial pressure to sustain combustion is important because the value can be directly compared with normoxic condition (21 kPa of oxygen partial pressure which is suitable condition for human living and indicated by the

green dashed line in Fig. 3) and hypoxic condition (16 kPa of oxygen partial pressure, represented by the blue dashed line in Fig. 3) that are required for human living. Figure 3 shows the extinction limit in terms of oxygen partial pressure (Limiting Oxygen Partial Pressure: LOPP) under different total ambient pressure conditions. The data are those displayed in Fig. 2 but plotted in the partial pressure-total pressure plane.

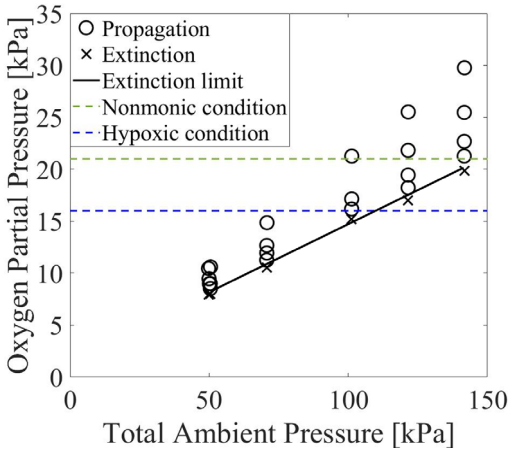

Fig. 3 Extinction limit in terms of oxygen partial pressure
(Flow velocity: 10 cm/s, opposed flow, microgravity)

According to Fig. 3, the LOPP decreased as total ambient pressure decreased. However, the trend of the LOPP is opposite from that of the LOC case. It means that high pressure region has an advantage from the perspective of human life because LOPP in low pressure region is always lower than hypoxic condition using this material.

4. Discussion and analysis

According to the previous section, the extinction limit using volumetric oxygen concentration (LOC) increased as total ambient pressure decreased. However, the extinction limit in terms of oxygen partial pressure (LOPP) decreased as total ambient pressure decreased. As just described, the trend

of extinction limit was changed as the y-axis was changed from oxygen concentration to oxygen partial pressure even with the same experimental observation. To explain these experimental trends, a scale analysis has been carried out referring to the heat balance model for flat sheet sample [33] considering wire sample geometry.

4.1. Model of flame spreading over electrical wire in opposed flow in microgravity

Figure 4 shows the schematic of a flame spread over a wire in opposed flow case. To discuss the physics in microgravity, we ignored the effect of natural convection, dripping of insulation and the direction of gravity, all of which need to be considered in normal gravity. The opposed flow velocity V_g is due to forced flow. With respect to the flame, the oxidizer, assumed to be a mixture of oxygen and nitrogen, approaches with a velocity V_g and the flame spread rate is referred to as V_f.

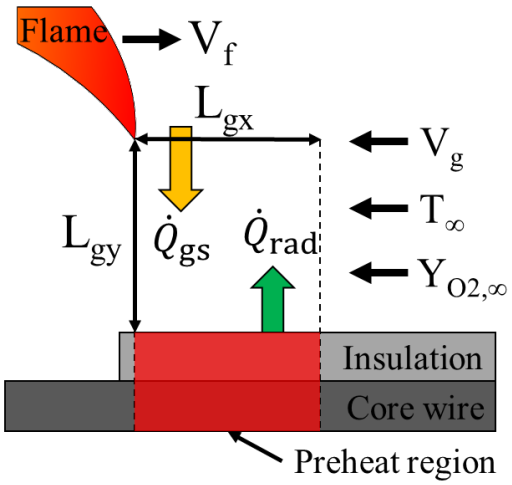

Fig. 4 Schematic of propagation flame in opposed flow

The following assumptions underlie this physical model: 1) The core and the insulation are thermally thin in the radial direction; 2) The shape of the insulation does not change within the preheat region; 3) Heat conduction through the wire core is ignored because a flame spreading over NiCr wire insulation is mainly governed by gas phase driven heat transfer [14]; 4) Flame reached steady state;

5) Both the wire core and the insulation are in perfect thermal contact. In this model, the preheat length (L_{gx}) and stand-off distance (L_{gy}) are important features to explain the flame spreading. According to past studies, the preheat length and stand-off distance are defined by the following equation [15]:

$$L_{gx} = L_{gy} = \frac{\alpha_g}{V_g} \tag{1}$$

where α_g is the gas thermal diffusivity. As ambient pressure decreases, preheat length and stand-off distance increase because gas density decreases. To calculate the extinction limit in Section 4.2 and 4.3, the preheat length and stand-off distance were assumed to be inversely proportional to the ambient pressure. Moreover, in the thermally thin case, heat balance equation in the preheat region leads to the following expression [17].

$$\dot{Q}_{gs} - \dot{Q}_{rad} = \dot{Q}_{req} \tag{2}$$

where $\dot{Q}_{gs}$, $\dot{Q}_{rad}$, and $\dot{Q}_{req}$ are the heat conduction rate from the flame to the wire insulation, radiation loss rate from the insulation surface to the ambient, and the energy to sustain the flame propagation, respectively. These heat quantities can be evaluated by the following equations [17]:

$$\dot{Q}_{gs} = \frac{2\pi\lambda_g(T_f - T_p)}{\ln(1 + L_{gy}/r_s)} L_{gx} \tag{3}$$

$$\dot{Q}_{rad} = 2\pi r_s \epsilon_s \sigma (T_p^4 - T_\infty^4) L_{gx} \tag{4}$$

$$\dot{Q}_{req} = V_f \pi \{r_c^2 \rho_c c_c + (r_s^2 - r_c^2)\rho_s c_s\}(T_p - T_\infty) \tag{5}$$

where r_s and r_c are the radius of the wire and the inner core, respectively; λ_g, ε_s and, σ are the thermal conductivity of the gas phase, the emissivity, and the Stefan-Boltzmann constant, respectively; T_f, T_p, and T_∞ are the flame temperature (assumed as the adiabatic flame one), the

pyrolysis temperature, and the ambient temperature; ρ and c are the density and the specific heat, respectively, while s and c denote the insulation and the core, respectively. To calculate the extinction limit in Section 4.2 and 4.3, pyrolysis temperature was assumed to be independent of the ambient pressure following the approach by Nakamura et al. [14]. Also, according to the calculated result by CEA2 (the NASA-equilibrium program to calculate adiabatic flame temperature) [34], the difference of adiabatic flame temperature is small over the experimental pressure range (less than 1 % change around the LOC value from experiments). Therefore, it was assumed to be independent of ambient pressure under constant oxygen concentration. Moreover, to discuss extinction phenomena, the following non-dimensional equation was used which is derived from Eq. (2).

$$1 = \mathrm{R_{loss}} + \eta \tag{6}$$

where $\mathrm{R_{loss}}$ and η are the radiation number for wire and a non-dimensional flame spread velocity which can evaluated by following equations:

$$\begin{aligned} \mathrm{R_{loss}} &= \dot{Q}_{rad}/\dot{Q}_{gs} \\ \eta &= \dot{Q}_{req}/\dot{Q}_{gs} \end{aligned} \tag{7}$$

To calculate the extinction limit in Section 4.2 and 4.3, when the $\mathrm{R_{loss}}$ reached the critical value, the flame was assumed to be extinguished. Theoretically, extinction should happen when $\mathrm{R_{loss}}$=1, independent of the pressure condition. In the literature, an empirical factor has been used in the treatment of the experimental data [33] , and a constant Rloss (lower than unity) was adopted herein as well.

4.2. The effect of ambient pressure on extinction limit using volumetric oxygen concentration

Figure 5 shows the calculation of LOC as a function of total ambient pressure using various R_{loss} value.

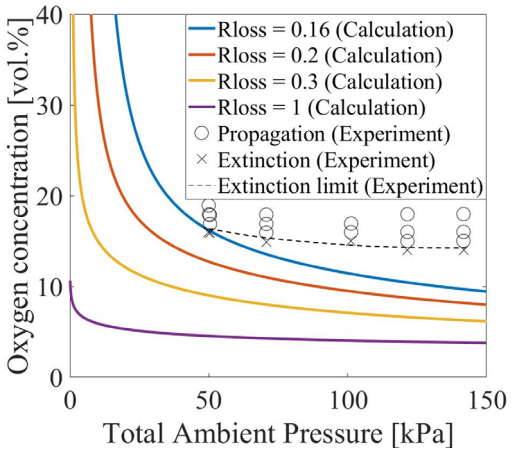

Fig. 5 Calculation result of extinction limit in terms of volumetric oxygen concentration

In Fig. 5, solid lines indicate the calculation results, while the black open circles, the black crosses, and the black dashed line are the experimental data as shown in Fig. 2 and taken in microgravity experiments. According to Fig. 5, the LOC by calculation increased as ambient pressure decreased regardless of R_{loss}, and this trend qualitatively matched the experimental data. This trend can be explained by radiation loss from wire surface. As the ambient pressure decreases, the preheat length increases. And, an increase in preheat length causes an increasing radiation loss from the wire surface. Finally, the increasing radiation loss causes the increase in LOC. That being said, the trend extracted from calculations had a large slope as compared to that of the experimental data and the difference between calculation and experiment became larger especially within the higher pressure region. One of the potential reasons of this difference is the omission of the core wire effect. This is because that characteristic preheat length of the wire core becomes larger than that of the gas phase in high pressure case as pointed out by Nakamura et al. [14]. When the oxygen concentration is close to the LOC, the

larger characteristic preheat length of the wire core could be a major heat loss mechanism, resulting that core wire act like a “heat sink” at higher pressure. The theoretical curve in Fig. 5 did not include such an effect.

This experimental fact gives new perspective for the design of spacecraft cabin atmosphere in terms of flammability limit. Figure 6 shows the basic bounding discussion for spacecraft atmosphere design from NASA/CR-2005-213689 [22].

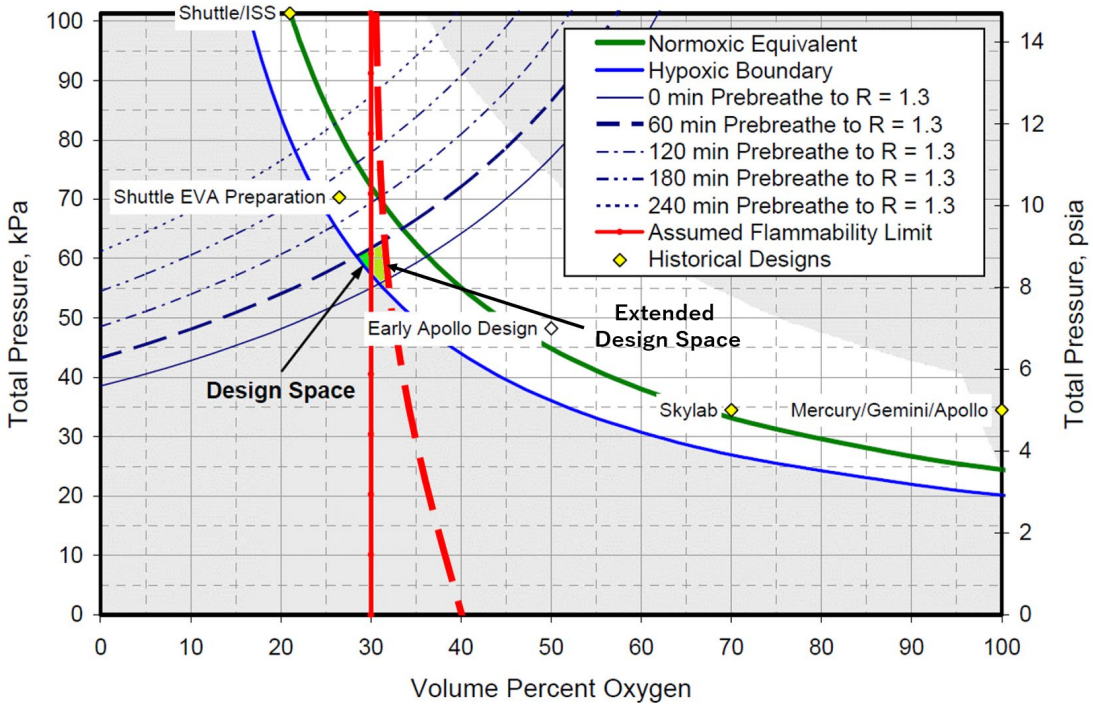

Fig. 6 Modified resultant spacecraft cabin atmosphere design space given by NASA/CR-2005-213689 [22]

In Fig. 6, green and blue lines indicate the normoxic and hypoxic conditions, respectively. These lines were drawn using the alveolar gas equation [22], which relates the oxygen partial pressure within the alveoli of the lung to the oxygen partial pressure within the breathing atmosphere (inspired air). Moreover, the five indigo lines including dashed line, dot line and so on indicate the necessary pre-breathe time under the spacecraft cabin atmosphere pressure and oxygen concentration to avoid

decompression sickness. In these lines, 60-minute line was set as an upper tentative bound on the pre-breathe time. Further discussion about the pre-breathe time is reported by NASA/CR-2005-213689 [22]. Finally, the red solid line indicates the current NASA maximum testing limit for general material use inside spacecraft habitable (cabin) areas. Currently, this line (30 % of oxygen concentration) is assumed as flammability limit by NASA/CR-2005-213689 [22]. Finally, the green area surrounded by hypoxic line, 60-minute pre-breathe line and flammability limit assumed as the ideal design space for spacecraft. However, this design region is quite narrow and further discussion is ongoing to enlarge this design space [22]. On this point, our experimental fact may give a new perspective in terms of flammability limit. The dashed red line indicates the assumed modified flammability limit based on our discussion. The modified flammability line increased as ambient pressure decreased, and this modification allow to enlarge the flammability limit especially towards lower-pressure region. Finally, the modified design space was extended as compared to the original one. This fact implies to extend the limitation based on the above bounding discussion and open the opportunity to enlarge the operational atmosphere condition of spacecraft design

4.3. The effect of ambient pressure on the extinction limit in terms of oxygen partial pressure

Figure 7 shows the calculation of LOPP as a function of total ambient pressure using various R_{loss} value.

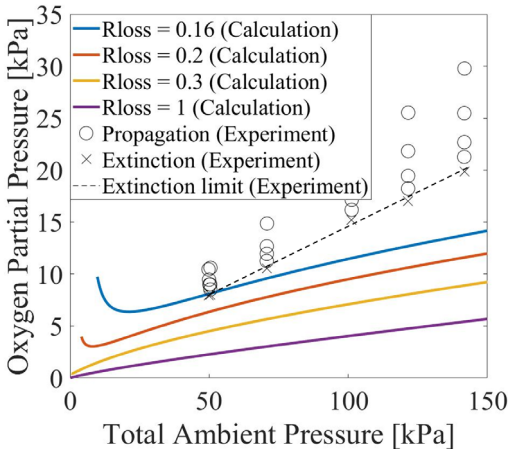

Fig. 7 Calculation result of extinction limit in terms of oxygen partial pressure

In Fig. 7, the solid lines indicate the calculation results, while the black open circles, the black crosses, and the black dashed line are the experimental data as displayed in Fig. 3 and taken in microgravity experiments. Again, the dataset shown in Fig. 7 is that shown in Fig. 5 but plotted in the partial pressure-total pressure plane. According to Fig. 7, the LOPP by calculation decreased as ambient pressure decreased over the experimental pressure range regardless of R_{loss}, and this trend qualitatively matched the experimental data. This trend can be explained by the flame temperature. When the ambient pressure decreased at constant oxygen partial pressure, the flame temperature increased because of the increase in oxygen concentration (or decrease in dilution gas content). The increasing flame temperature then causes the increase in heat release from the flame to the wire insulation. Finally, the increase in heat release causes a decrease in LOPP as the ambient pressure is decreased. However, as the ambient pressure further decreased, the LOPP again could increase especially when the small R_{loss} value is assumed because of the increase in radiative heat loss from the wire surface such as in the case of LOC. However, to observe this reversal trend phenomenon, conditions leading to large radiative heat loss could be necessary, such as flat sheet sample, high pyrolysis temperature

material, or small external flow velocity condition (such as in microgravity).

5. Conclusions

The effect of ambient pressure on the extinction limit of a flame spreading over a wire insulation in an opposed flow in microgravity was studied experimentally. Low-density polyethylene insulated Nickel-Chrome wires was used to investigate the extinction phenomena at various ambient pressure levels. The experimental observations showed that the extinction limit using volumetric oxygen concentration (LOC) increased with decreasing ambient pressure over the pressure range investigated. Moreover, when the data was plotted in partial pressure-total pressure plane, the extinction limit of oxygen partial pressure (LOPP) decreased with decreasing ambient pressure over the pressure range investigated. In terms of LOC consideration, the reason for this trend is attributed to the radiation heat loss that increases as the ambient pressure decreased. Moreover, in terms of LOPP consideration, the reason for this trend is the increase in the flame temperature within the lower pressure region. Considering the above findings, high pressure region is suitable for manned spacecraft using the consideration of normoxic and hypoxic boundary. Moreover, this result implies that there is a possibility to enlarge the range of operational conditions in the design of spacecraft based on the bounding discussion for spacecraft atmosphere design by accounting for the effect of ambient pressure on flammability limit.

Acknowledgments

This research is supported by Japan Space Exploration Agency (JAXA) under the project of FLARE and the Centre National d'Etudes Spatiales (CNES) under contract #130615. The support from the topical team on fire safety in space (ESA-ESTEC contract number 4000103397) is also appreciated. The authors appreciate the contributions of Renaud Jalain and Ulises Rojas Alva during the parabolic flight experiments.

References

[1] R. Friedman, Fire Safety in Spacecraft, *Fire Mater.* 20 (5) (1996) 235–243.

[2] S. Takahashi, M. A. F. bin Borhan, K. Terashima, A. Hosogai, and Y. Kobayashi, Flammability limit of thin flame retardant materials in microgravity environments, *Proc. Combust. Inst.* 37 (3) (2018) 4257–4265.

[3] S. Link, X. Huang, C. Fernandez-Pello, S. Olson, and P. Ferkul, The Effect of Gravity on Flame Spread over PMMA Cylinders, *Sci. Rep.* 8 (1) (2018) 120.

[4] O. Fujita, T. Kyono, Y. Kido, H. Ito, and Y. Nakamura, Ignition of electrical wire insulation with short-term excess electric current in microgravity, *Proc. Combust. Inst.* 33 (2) (2011) 2617–2623.

[5] Y. Takano, O. Fujita, N. Shigeta, Y. Nakamura, and H. Ito, Ignition limits of short-term overloaded electric wires in microgravity, *Proc. Combust. Inst.* 34 (2) (2013) 2665–2673.

[6] K. Shimizu, M. Kikuchi, N. Hashimoto, and O. Fujita, A numerical and experimental study of the

ignition of insulated electric wire with long-term excess current supply under microgravity, *Proc. Combust. Inst.* 36 (2) (2017) 3063–3071.

[7] O. Fujita, M. Kikuchi, K. Ito, and K. Nishizawa, Effective mechanisms to determine flame spread rate over ethylene-tetrafluoroethylene wire insulation: Discussion on dilution gas effect based on temperature measurements, *Proc. Combust. Inst.* 28 (2) (2000) 2905–2911.

[8] O. Fujita, K. Nishizawa, and K. Ito, Effect of low external flow on flame spread over polyethylene-insulated wire in microgravity, *Proc. Combust. Inst.* 29 (2) (2002) 2545–2552.

[9] J. M. Citerne, H. Dutilleul, K. Kizawa, M. Nagachi, O. Fujita, M. Kikuchi, G. Jomaas, S. Rouvreau, J. L. Torero, and G. Legros, Fire safety in space – Investigating flame spread interaction over wires, *Acta Astronaut.* 126 (2016) 500–509.

[10] M. Kikuchi, O. Fujita, K. Ito, A. Sato, and T. Sakuraya, Experimental study on flame spread over wire insulation in microgravity, *Symp. Combust.* 27 (2) (1998) 2507–2514.

[11] M. K. Kim, S. H. Chung, and O. Fujita, Effect of AC electric fields on flame spread over electrical wire, *Proc. Combust. Inst.* 33 (1) (2011) 1145–1151.

[12] S. J. Lim, M. Kim, J. Park, O. Fujita, and S. Chung, Flame spread over electrical wire with AC electric fields: Internal circulation, fuel vapor-jet, spread rate acceleration, and molten insulator dripping, *Combust. Flame* 162 (4) (2015) 1167–1175.

[13] S. Takahashi, H. Takeuchi, H. Ito, Y. Nakamura, and O. Fujita, Study on unsteady molten insulation volume change during flame spreading over wire insulation in microgravity, *Proc. Combust. Inst.* 34 (2) (2013) 2657–2664.

[14] Y. Nakamura, N. Yoshimura, H. Ito, K. Azumaya, and O. Fujita, Flame spread over electric wire in sub-atmospheric pressure, *Proc. Combust. Inst.* 32 II (2) (2009) 2559–2566.

[15] Y. Konno, N. Hashimoto, and O. Fujita, Downward flame spreading over electric wire under various oxygen concentrations, *Proc. Combust. Inst.* 37 (3) (2019) 3817–3824.

[16] M. Nagachi, F. Mitsui, J. M. Citerne, H. Dutilleul, A. Guibaud, G. Jomaas, G. Legros, N. Hashimoto, and O. Fujita, Can a spreading flame over electric wire insulation in concurrent flow achieve steady propagation in microgravity?, *Proc. Combust. Inst.* 37 (3) (2019) 4155–4162.

[17] S. Takahashi, H. Ito, Y. Nakamura, and O. Fujita, Extinction limits of spreading flames over wires in microgravity, *Combust. Flame* 160 (9) (2013) 1900–1902.

[18] K. Mizutani, K. Miyamoto, N. Hashimoto, Y. Konno, and O. Fujita, Limiting Oxygen Concentration Trend of ETFE-Insulated Wires under Microgravity, *Int. J. Microgravity Sci. Appl* 35 (1) (2018) 350104.

[19] A. F. Osorio, K. Mizutani, C. Fernandez-Pello, and O. Fujita, Microgravity flammability limits of ETFE insulated wires exposed to external radiation, *Proc. Combust. Inst.* 35 (3) (2015) 2683–2689.

[20] M. Nagachi, F. Mitsui, J.-M. Citerne, H. Dutilleul, A. Guibaud, G. Jomaas, G. Legros, N. Hashimoto, and O. Fujita, Effect of Ignition Condition on the Extinction Limit for Opposed Flame Spread Over Electrical Wires in Microgravity, *Fire Technol.* (2019).

[21] O. Fujita, Solid combustion research in microgravity as a basis of fire safety in space, *Proc. Combust. Inst.* 35 (3) (2015) 2487–2502.

[22] K. E. Lange, A. T. Perka, B. E. Duffield, and F. F. Jeng, Bounding the Spacecraft Atmosphere

Design Space for Future Exploration Missions, *Nasa/Cr* (June 2005) (2005) 213689.

[23] A. F. J. Abercromby, B. K. Alpert, J. S. Cupples, E. L. Dillon, A. Garbino, Y. Hernandez, C. Kovich, M. J. Miller, J. Norcross, C. W. Pittman, S. Rajulu, and R. A. Rhodes, Integrated Extravehicular Activity Human Research Plan: 2019, *Nasa/Tr* (July) (2019).

[24] L. K. HONDA and P. D. RONNEY, Effect of Ambient Atmosphere on Flame Spread at Microgravity, *Combust. Sci. Technol.* 133 (4–6) (1998) 267–291.

[25] M. Thomsen, X. Huang, C. Fernandez-Pello, D. L. Urban, and G. A. Ruff, Concurrent flame spread over externally heated Nomex under mixed convection flow, *Proc. Combust. Inst.* 37 (3) (2019) 3801–3808.

[26] M. Thomsen, D. C. Murphy, C. Fernandez-pello, D. L. Urban, and G. A. Ruff, Flame spread limits (LOC) of fire resistant fabrics, *Fire Saf. J.* 91 (May) (2017) 259–265.

[27] A. C. FERNANDEZ-PELLO and T. HIRANO, Controlling Mechanisms of Flame Spread, *Combust. Sci. Technol.* 32 (1–4) (1983) 1–31.

[28] A. E. Frey and J. S. T'ien, Near-limit flame spread over paper samples, *Combust. Flame* 26 (C) (1976) 257–267.

[29] J. Fang, Y. Zhang, X. Huang, Y. Xue, J. Wang, S. Zhao, X. He, and L. Zhao, Dripping and Fire Extinction Limits of Thin Wire: Effect of Pressure and Oxygen, *Combust. Sci. Technol.* 00 (00) (2019) 1–16.

[30] A. Guibaud, J. M. Citerne, J. M. Orlac'H, O. Fujita, J. L. Consalvi, J. L. Torero, and G. Legros, Broadband modulated absorption/emission technique to probe sooting flames: Implementation,

validation, and limitations, *Proc. Combust. Inst.* 37 (3) (2019) 3959–3966.

[31] A. Guibaud, J. M. Citerne, J. L. Consalvi, O. Fujita, J. Torero, and G. Legros, Experimental Evaluation of Flame Radiative Feedback: Methodology and Application to Opposed Flame Spread Over Coated Wires in Microgravity, *Fire Technol.* (2019).

[32] A. Guibaud, J. L. Consalvi, J. M. Orlac'h, J. M. Citerne, and G. Legros, Soot Production and Radiative Heat Transfer in Opposed Flame Spread over a Polyethylene Insulated Wire in Microgravity, *Fire Technol.* (2019).

[33] S. Takahashi, M. Hotta, S. Bhattacharjee, T. Ihara, and K. Wakai, Classification of Flame Spread Behavior over a Solid Material by Scale Analysis, *Int. J. Microgravity Sci. Appl.* 29 (1) (2012) 23–31.

[34] S. Gordon and B. J. McBride, Computer Program for Calculation of Complex Chemical Equilibrium Compositions and Applications I. Analysis, *NASA Ref. Publ.* 1311 (1994).

Figure Captions

Fig. 1 Backlighted images of opposed flame spread over wire insulation at different ambient pressures

(21 % of oxygen concentration, 100 mm/s of external flow velocity)

Fig. 2 Extinction limit using volumetric oxygen concentration

(Flow velocity: 10 cm/s, opposed flow, microgravity)

Fig. 3 Extinction limit in terms of oxygen partial pressure

(Flow velocity: 10 cm/s, opposed flow, microgravity)

Fig. 4 Schematic of propagation flame in opposed flow

Fig. 5 Calculation result of extinction limit in terms of volumetric oxygen concentration

Fig. 6 Modified resultant spacecraft cabin atmosphere design space given by NASA/CR-2005-213689 [22]

Fig. 7 Calculation result of extinction limit in terms of oxygen partial pressure